Title
SHELL EFFECTS AT HIGH SPIN IN THE Y-CONTINUUM FROM TE EVAPORATION RESIDUES

Author
Simon, R.S.

Publication Date
1978

Submitted to Nuclear Physics

LBL-6531
Preprint C.

SHELL EFFECTS AT HIGH SPIN IN THE γ-CONTINUUM FROM TE EVAPORATION RESIDUES

R. S. Simon, R. M. Diamond, Y. El Masri,
J. O. Newton, P. Sawa, and F. S. Stephens

January 1978

Prepared for the U. S. Department of Energy
under Contract W-7405-ENG-48

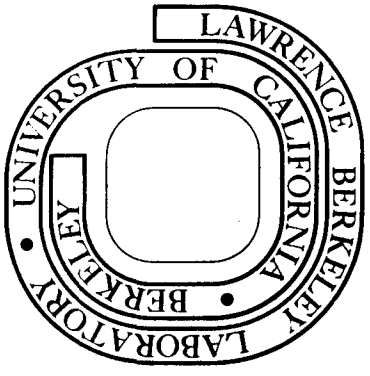

DISCLAIMER

SHELL EFFECTS AT HIGH SPIN IN THE γ-CONTINUUM FROM TE EVAPORATION RESIDUES[+]

R. S. Simon,[*] R. M. Diamond, Y. El Masri,[**] J. O. Newton,[†] P. Sawa,[††] and F. S. Stephens
Nuclear Science Division
Lawrence Berkeley Laboratory
University of California
Berkeley, California 94720

ABSTRACT

The continuum γ-ray spectra following $^{110}Pd(^{12}C,xn\gamma)Te$ and $^{82}Se(^{40}Ar,xn\gamma)Te$ reactions at several bombarding energies have been measured. As in earlier studies, the spectra show three main components: 1) discrete transitions in the ground band, 2) an yrast "bump", 3) a high-energy statistical tail. In addition, there appears to be a minimum in the spectrum before the yrast bump. The existence of this minimum and of the two peaks of discrete γ-ray transitions indicate a non-rotational structure for the nuclei at low spin ($\leq$ 30) before changing at higher spin to the rotational behavior suggested by the bump itself. Theoretical calculations including shell effects do show this type of behavior.

[+]This work was supported by the Division of Nuclear Physics of the Department of Energy

[*]Gesellschaft für Schwerionenforschung, Darmstadt, Germany

[**]Institut de Physique Corpusculaire, Louvair-la-Neuve, Belgium

[†]The Australian National University, Canberra, A.C.T. 2600, Australia

[††]Research Institute for Physics, Stockholm, Sweden

NUCLEAR REACTIONS ^{82}Se (^{40}Ar, xnγ), E = 161, 174, 185 MeV and ^{110}Pd (^{12}C, xnγ), E = 53, 78, 105 MeV; measured E_γ, γ-ray multiplicities. ^{118}Te deduced spins, moments of inertia, change in nuclear structure. Enriched targets.

1. Introduction

The liquid-drop model of the nucleus is a simple and convenient representation capable of explaining many of the macroscopic properties of nuclei, although it cannot give all details. For example, it was used to explain the fission process[1]), but fails to account for asymmetric fission; it was able to describe the major features of the nuclear potential energy surface[2]), but only the addition of shell corrections[3,4]) brings the energy-surface calculations into good agreement with experimental results. This shell structure is related to the spacing or bunching of the single-particle levels at the Fermi surface, and it plays a major role in determining the properties of nuclei near the ground state. Doubly-even nuclei at closed shells have a large spacing to the next available orbital and are spherical or near-spherical. In contrast, nuclei between shell closings usually have a relatively high level density at their Fermi surface and tend to be deformed.

As angular momentum is added to a nucleus, it may stretch, depending upon how steeply the potential rises with deformation, but more importantly, the various Nilsson orbitals are expected to move with respect to each other depending upon their Ω values[4]). Thus the level density at the Fermi surface changes as a function of the angular momentum. This variation in the bunching of the single-particle levels will shift the shell closures and may cause marked shape changes in the nucleus at certain (higher) spins. In fact, it is thought that shell effects will continue to occur up to high spins with comparable magnitudes, but there has been little experimental evidence on this point.

At the present time most of our information on the properties of states in the angular-momentum range above 25ħ comes from investigations on heavy ion, xn reaction[5-11]). The γ-ray spectra observed three main components: 1) the discrete transitions of the ground band, usually below 1 MeV in energy; 2) a broad unresolved bump of transitions extending to somewhat higher energy made up of the members of the collective cascades parallel to the yrast line; and 3) a component of unresolved γ-rays which goes to considerably higher energy, but decreases approximately exponentially in intensity with energy. This last group is thought to consist of the statistical transitions which lead to movement towards the yrast line.

In this paper we report on an investigation of the γ-continuum from the decay of Te evaporation residues, in which we observe additional finer structure for the first time. This structure may be interpreted as evidence for shell effects in these nuclei at high angular momentum and is compared to results from recent microscopic calculations.

2. Experimental Procedure and Analysis

The ^{122}Te system was produced via ^{110}Pd + ^{12}C and ^{82}Se + ^{40}Ar reactions with ~ 7mg/cm^2 self-supporting and ~ 1mg/cm^2 lead-backed targets, respectively. The initial projectile energies were 53,78, and 105 MeV for the ^{12}C bombardments and 161,174, and 185 MeV for the ^{40}Ar ones. Considering the target thicknesses, these lead to average bombarding energies in the targets of 50,75, and 102 MeV and 157,170, and 181 MeV for the ^{12}C and ^{40}Ar runs, respectively. Projectile energies given hereafter will refer to such average energies in the targets unless explicitly stated otherwise. The decay γ-radiation was observed in four 7.5 cm × 7.5 cm NaI(Tl)

detectors placed at 0°, 30°, 60° and 90° to the beam direction and 60 cm from the target. These detectors were gated by coincident pulses in a Ge detector in order to select continuum γ-spectra associated with individual xn reaction channels as described previously.[5,6] Due to the fractionation of the total angular momentum, these γ-spectra for different reaction channels correspond to different angular-momentum ranges.

A Ge singles spectrum from the $^{82}Se + ^{40}Ar$ reaction at 157 MeV is shown in Fig. 1. The γ-lines from the Te reaction products are indicated, as well as the $2^+ \rightarrow 0^+$ transition in ^{114}Sn which corresponds to the strongest αxn channel. Since most of the Sn population is delayed in low-lying isomeric states, such Sn lines also appear in the out-of-beam part of the spectrum. The αxn cross section is significant with ^{40}Ar beams at 157 MeV bombarding energy, and becomes approximately equal to the pure xn cross section at 181 MeV. The Ge spectrum from the 157 MeV reaction taken in prompt coincidence with γ-rays in the 0° NaI detector is shown in Fig. 2. The energy range selected contains most of the intense xn lines. The background in the spectrum is mainly due to Compton events from the high-energy transitions in the continuum part of the γ-decay.

The discrete transitions in ^{118}Te above the previously known 8^+ state have been identified in a separate experiment. There we have measured excitation functions for the $^{110}Pd + ^{12}C$ reaction and studied angular distributions and γ-γ coincidences at 70 MeV bombarding energy with two Ge detectors placed at 0° and 90° with respect to the beam direction. The decay scheme suggested by these results is given in Fig. 3.

From the raw NaI spectra corresponding to the individual xn channels the true γ-distributions were obtained by unfolding[6,13]). As an example, the pulse-height and unfolded spectra obtained in the $^{82}Se(^{40}Ar,4n)\ ^{118}Te$ reaction at 181 MeV are shown in Fig. 4. When we unfold a spectrum with poor statistics as here, very large and unrealistic fluctuations in the resulting γ-ray spectrum may appear. They arise because at high incident γ-ray energy only a small fraction of the NaI pulse-height distribution is in the full-energy peak; a large fraction is in the Compton distribution. But from the observed Ge spectra we know that discrete lines with significant intensities are not usually seen at energies $\gtrsim$ 1 MeV in these Te spectra. It therefore seems likely that the NaI spectra for energies > 1 MeV will be fairly smooth. We have made this assumption and for each raw spectrum have drawn a number of smooth lines through the data points, consistent with their errors and keeping the integral of the counts approximately constant. These smoothed lines were unfolded and a somewhat better estimate of the true γ-ray distribution and its errors obtained than by directly unfolding the original data. The line in the raw data in the lower part of Fig. 4 is that judged to be the best fit. Unfolding this and comparing with the singles spectrum gives the γ-spectrum in transitions per 40 keV shown in the upper spectrum. Errors on this are also indicated. Care must be taken in interpreting these individual errors, since they are correlated due to the unfolding procedure. It should be appreciated that the error in the total area of, say, the 1.2 - 2.3 MeV bump is fairly small, but that some variation of the distribution of this area is allowed. It should also be mentioned that, because of poor statistics in this and some other cases, the slope of

the statistical part of the spectrum beyond about 2.8 MeV was assumed to be the same as that in the gross spectra, i.e., the spectra in coincidence with all the events from the Ge detector. In all cases the assumed lines were statistically consistent with this assumption. Although we cannot be certain that this procedure is correct, it may well be, since the slope of the gross spectrum was essentially independent of ^{40}Ar bombarding energy for medium and high energies and was the same in the ^{12}C-induced reaction at 75 MeV. Even if this assumption were only approximately correct, it would make little difference to the results which we shall discuss later, since there are so few γ-rays in the statistical as compared with the yrast cascade spectra.

The three components of the γ-spectrum mentioned in the introduction seem to be well established in the unfolded spectrum of Fig. 4: (1) the sharp peaks around 600 and 800 keV arise from the lowest seven discrete transitions in the ground band of ^{118}Te (best seen in the Ge spectra); (2) the large bump above 1.2 MeV with an upper edge around 2.3 MeV represents the collective cascades along the yrast region; and (3) the roughly exponentially decreasing tail at still higher energies is interpreted as part of the statistical cascade. But the yrast bump appears to be much reduced or missing altogether at the lower angular momenta brought in with the ^{12}C bombardments, as shown for the 4n channel in Fig. 5. The changes in the yrast bump region for the 4n,5n, and 6n channels are shown in Fig. 6 for both the 157 and 181 MeV ^{40}Ar reactions.

The anisotropy of the γ-radiation, plotted above the unfolded spectrum in Fig. 4, confirms the stretched-E2 character of the bump region. Integration of the total spectrum gives the average γ-ray multiplicity, $\bar{N}_\gamma$, after taking into account the gating transition in

the Ge detector and correcting for multiple coincidences which have been suppressed electronically. The γ-ray multiplicities of all the Te nuclei studied are given in Table 1. From these numbers an estimate of the average angular momentum carried off by the γ-ray cascades can be obtained. First one must subtract the intensity in the exponential tail and in its continuation as a statistical background underneath the yrast bump. This intensity δ corresponds to approximately four transitions. Then assuming these latter transitions carry off no net angular momentum (not completely true), we can estimate the average angular momentum in the γ-ray cascades for a particular channel from the expression $\bar{I}_\gamma = 2(\bar{N}_\gamma - \delta)$, tested in ref. 6. For the lowest xn reaction observed, the maximum angular momentum obtained is only a little higher than the average value, so, for example, with $\delta = 4$ we have, on the average, 27 ± 3 transitions in the γ-ray cascades for the 4n channel at 181 MeV, indicating a maximum spin somewhere near $60\hbar$.

3. Discussion

From the liquid-drop model one finds that a rigidly rotating, charged drop prefers an oblate shape until shortly prior to the point where it breaks apart under the centrifugal force[2]). At very high angular momenta, just below values leading to fission, the nucleus is predicted to stretch out into very deformed (triaxial) shapes. A schematic view of the full range of angular momenta expected for a nucleus of mass $A \simeq 122$ is given in Fig. 7, where excitation energy is plotted vs. angular momentum. The lower, approximately parabolic, line is the yrast line, which represents the ground state of the rotating nucleus. The upper line corresponds

to the rotating saddle-point configuration, and the difference between these lines represents the fission barrier at that value of spin. Fission is expected to become observable when the barrier drops below 8-10 MeV and this or the onset of α-particle emission will determine the effective maximum angular momentum that can be studied in the γ-decay of such a nucleus. A recent survey[14]) of multiplicity distributions of the γ-ray cascades following heavy-ion xn reactions over a broad range of the periodic table has confirmed the results of simple calculations which indicate that α-emission will establish this limiting angular momentum for products with $Z \lesssim 60$ and fission will do so for $Z \gtrsim 60$. On this basis, the Te system chosen seems to be rather favorably placed for populating very high angular-momentum states.

Tellurium nuclei are spherical or weakly deformed near the ground state (the stable Te nuclei have slightly prolate 2^+ states[15]) as a result of nuclear shell structure, namely the closed proton shell at $Z = 50$. However, at high spins the classical liquid-drop effects are predicted to drive these nuclei oblate though one must keep in mind the possible effect of shell corrections. Experimentally, information about the high-spin states observed in the Te nuclei produced in the present study is contained in the continuum spectra of the few-n reactions for example, the 4n channel in the $^{82}Se + ^{40}Ar$ reaction at 181 MeV (Fig. 4). It is compared with those for other reaction channels in Fig. 6, and with those for the 4n channel from the ^{40}Ar and from the ^{12}C reactions at several projectile energies in Fig. 5.

Several comments can be made as a result of these comparisons. From Fig. 6 we see that the absence of structure below ~ 1 MeV for the odd-mass

nucleus indicates there is no grouping of discrete transitions in this energy range for ^{117}Te, in contrast to the cases of the doubly-even nuclei ^{116,118}Te. More importantly, it is clear in Fig. 5 when comparing the spectra from the ^{12}C reactions with that from the 157 MeV ^{40}Ar irradiation that the size of the yrast bump in the spectrum develops with increasing angular momentum input to the compound system. This development of the bump suggests that these transitions arise from rotational cascades, as recently suggested in studies of the continuum γ-rays from Yb nuclei produced in a wide range of angular momenta by ^{16}O, ^{40}Ar, and ^{86}Kr reactions[6]). But while the bump increased regularly with angular momentum in all Yb cases the situation seems to be somewhat different for Te.

First of all, the yrast bump in Te appears only after a certain amount of angular momentum is brought into the system. This is shown by the ^{12}C,4n spectra in Fig. 5. From the measured average γ-ray multiplicities we can estimate the threshold angular momentum for the onset of the bump. Using the sharp cut-off model and assuming that the total angular-momentum distribution is fractionated into sharp bins for each reaction product we obtain a value around 30 $\hbar$.

Then with increasing angular-momentum uptake, the bump develops regularly at first. In Fig. 6 its upper edge is seen to move to higher transition energies if one follows the sequence from the 6n channel spectrum to the 5n one at 157 MeV to the 6n and 5n-channel spectra at 181 MeV and the 4n channel spectrum at 157 MeV. This corresponds to the behavior previously observed in Yb nuclei and suggests (as discussed there) the existence of regular rotational bands in this spin region.

In ^{162}Yb it was possible to correlate the edge energy with the maximum angular momentum at the top of the γ-ray cascade and thus to determine the moment of inertia of this nucleus at very high spin. Similarly, we can obtain moments of inertia in Te. The average γ-ray multiplicities of the 5n reaction at 181 MeV and the 4n channel at 157 MeV agree within the errors of our measurement and probably correspond to a maximum angular momentum around 55ħ in each of the γ-cascades. Together with the edge energy of 2.3 MeV we find a moment of inertia of $2\mathcal{I}/\hbar^2 = 95$ MeV^{-1}, compared to a rigid-sphere value of 85 MeV^{-1} and a liquid-drop estimate of about 100 MeV^{-1}.

At still higher input angular momenta the energy of the edge of the yrast bump no longer moves much. This can be seen in Fig. 5 if one compares the ^{40}Ar,4n spectra at 157,170, and 181 MeV average bombarding energy. Since the 4n reaction at 157 MeV already corresponds to a maximum angular momentum of ~ 55 ħ, and the maximum spin that can be held in the compound nucleus is of the order of 60ħ, little more angular momentum can be brought to the γ-ray cascades with increasing ^{40}Ar energy. So, little further movement of the edge is expected; a limiting situation is being approached and additional input angular momentum will lead to other exit channels (these are likely to involve α-particle emission). This is in agreement with the observed increasing population of αxn channels as the bombarding energy is raised, and is also plausible from the reduction in γ-ray multiplicity observed for the sum of all reactions at

181 MeV ^{40}Ar compared to 170 MeV. However, another possible explanation for the limited movement of the edge at these high spins is that a back-bend is taking place. At present we cannot say much about this from our data, so that we cannot decide between these possibilities.

In contrast, the behavior of Te at moderate spins seems to be more readily understood. Thus the two peaks observed at γ-ray energies of $\sim$ 600 and ~800 keV in the even-n spectra represent peculiarities in the nuclear structure that lead to the existence of several levels, roughly equally-spaced at those energies (see Fig. 3). In addition, there appears to be a minimum in the ^{40}Ar spectra between the 800 keV peak and the yrast bump. These factors argue against the existence of deformed rotational bands as the collective mode of excitation at spins much below 30$\hbar$. A relationship between transition energy and spin different from the rigid-rotor one is necessary to explain these data. The appearance of the bump then indicates a change to collective rotational behavior and is a reflection of changes in nuclear structure (shell effects) caused by the increasing angular momentum.

Recently, shell effects have been included in theoretical calculations[4,16,17] for nuclei at very high angular momentum by using a Strutinsky-smearing type of approach. In particular, Faessler and Ploszajcak[16] and Ragnarsson and Soroka[17] have calculated the transition energies between the yrast states of ^{118}Te for $I > 20$ with the assumption that pairing has broken down. The results from Ragnarsson and Soroka are shown in a plot of transition energy versus spin in Fig. 8, along with a curve representing the liquid-drop values for an A = 118 nucleus and the lowest known transitions in ^{118}Te. It is the slope in such a plot

that should compare inversely with the height of the Te spectrum of Fig. 4, if the feeding into the yrast region is mainly complete. The sharp rise in the calculated values of the transition energies around I = 26 would produce a valley in the γ-ray spectrum at that spin (at $E_\gamma \sim 1.3$ MeV), and the decrease and flatter slope thereafter would give a bump at a somewhat higher energy. This bump, caused in the calculation by an oblate to triaxial (prolate) shape change, comes at an energy somewhat comparable with the experimental one, but we should not expect too close a correspondence. The theoretical calculations refer to the γ-transitions between the yrast states, while the experimental results include not only the yrast cascade but also many sets of cascades in a region possibly several MeV wide above the yrast line. However, the important feature is that for the first time experimental results, namely the irregular behavior of the spectral intensity below 1.2 MeV in these Te nuclei and the large bump of intensity of higher energy (up to ~ 2.3 MeV) which appears at moderately high spins (> 30ħ), require shell effects to be considered.

It is not clear at the present time whether the correspondence between the experimental spectra and the results from the microscopic calculations for ^{118}Te are real or fortuitous, but it is clear that the accuracy and sensitivity of both experiment and calculation are approaching the point where meaningful comparisons can be made. Certainly the different behavior of the Te spectra as compared to the Yb ones shows that shell-structure effects continue to play an important role as the spin is increased. The exact cause and nature of the collective transition-energy limit seen at very high spin in these

Te spectra remain to be determined, but the observation of such behavior suggests that investigation of other nuclei at high spin will demonstrate additional structure effects.

Acknowledgments

We would like to thank Drs. I. Ragnarsson and D. P. Soroka for interesting and helpful discussions on nuclei at high spin, and Dr. I-Y Lee for help with certain phases of the experiments. We are indebted to the operating crew of the 88" Cyclotron for providing the beams used in this study, and to Mr. Mon Lee and Mr. Don Lebeck for help with the electronics and the computer, respectively.

References

1. N. Bohr and J. A. Wheeler, Phys. Rev. 56 (1939) 426.
2. S. Cohen, F. Plasil, and W. J. Swiatecki, Ann. of Phys. (New York) 82 (1974) 557.
3. V. M. Strutinsky, Nucl. Phys. A95 (1967) 420.
4. G. Andersson, S. E. Larson, G. Leander, P. Möller, S. G. Nilsson, I. Ragnarsson, S. Åberg, R. Bengtsson, J. Dudek, B. Nerlo-Pomorska, K. Pomorski, and Z. Symanski, Nucl. Phys. A262 (1976) 205; A. Bohr and B. R. Mottelson, Physica Scripta 10A (1974) 13.
5. P. Tjøm, F. S. Stephens, R. M. Diamond, J. de Boar, and W. E. Meyerhof, Phys. Rev. Lett. 33 (1974) 593; M. V. Banaschik, R. S. Simon, P. Colombani, D. P. Soroka, F. S. Stephens, and R. M. Diamond, Phys. Rev. Lett. 34 (1975) 892; R. S. Simon, M. V. Banaschik, P. Colombani, D. P. Soroka, F. S. Stephens, and R. M. Diamond, Phys. Rev. Lett. 36 (1976) 359.
6. R. S. Simon, M. V. Banaschik, R. M. Diamond, J. O. Newton, and F. S. Stephens, Nucl. Phys.
7. E. der Mateosian, O. C.Kistner, and A. W. Sunyar, Phys. Rev. Lett. 33 (1974) 596.
8. J. O. Newton, J. C. Lisle, G. D. Dracoulis, J. R. Leigh, and D. C. Weisser, Phys. Rev. Lett. 34 (1975) 99.
9. G. B. Hagemann, R. Broda, B. Herskind, M. Ishihara, S. Ogaza, and H. Ryde, Nucl. Phys. A245 (1975) 166; O. Andersen, R. Bauer, G. B. Hagemann, M. L. Halbert, B. Herskind, M. Neiman, and H. Oeschler, Nucl. Phys.

10. M. Fenzl and O.W.B. Schult, Z. Physik 272 (1975) 207.

11. D. G. Sarantites, J. H. Barker, M. L. Halbert, D. C. Hensley, R. A. Dagras, E. Eichler, N. R. Johnson, and J. A. Gronemeyer, Phys. Rev. C14 (1976) 2138.

12. W. Trautman, D. Proetel, O. Häusser, W. Hering, and F. Riess, Phys. Rev. Lett. 35 (1975) 1694.

13. J. F. Mollenauer, Phys. Rev. 127 (1962) 867.

14. J. O. Newton, I. Y. Lee, R. S. Simon, M. M. Aleonard, Y. El-Masri, F. S. Stephens, and R. M. Diamond, Phys. Rev. Lett. 38 (1977) 810.

15. A. M. Kleinfeld, G. Mäggi, and D. Werdecker, Nucl. Phys. A248 (1975) 342.

16. A. Faessler and M. Ploszajcak, private communication, 1977.

17. I. Ragnarsson and D. P. Soroka, private communication, 1976.

Table 1 Average γ-ray multiplicities for evaporation residues from ^{122}Te.

Reaction		Channel	$\bar{N}_\gamma$ [a]
$^{110}Pd + ^{12}C$	50 MeV	3n	8 ± 1
		4n	7 ± 1
	75 MeV	4n	19 ± 2
		5n	11 ± 1
	102 MeV	6n	16 ± 2
$^{82}Se + ^{40}Ar$	157 MeV	4n	26 ± 3
		5n	18 ± 2
		6n	14 ± 1
	170 MeV	4n	28 ± 3
		5n	22 ± 2
		6n	18 ± 2
	181 MeV	4n	31 ± 3
		5n	24 ± 2
		6n	20 ± 2

a) The average angular momentum of the γ-decay can be calculated from the relation $\bar{I}(\gamma) = 2(\bar{N}_\gamma - 4)$. For the 5n product ^{117}Te we add $^{11}/_2$ to account for the spin of the $h_{11/2}$ band head (the gating transitions for the NaI spectra belong to the $h_{11/2}$ band; the $^{11}/_2$-state is isomeric).

Figure Captions

Fig. 1 Ge singles spectra in-beam and out-of-beam (20 - 60 ns after the beamburst) for $^{82}Se + ^{40}Ar$ at 157 MeV.

Fig. 2 Ge spectrum in coincidence with the 0° NaI counter for $^{82}Se + ^{40}Ar$ at 157 MeV.

Fig. 3 Partial level scheme of ^{118}Te.

Fig. 4 NaI pulse-height spectrum for $^{82}Se + ^{40}Ar \rightarrow ^{118}Te + 4n$ at 118 MeV, and the corresponding unfolded spectrum. The pulse-height spectrum is the sum from all four detectors at 0°, 30°, 60° and 90° and is close to the isotropic average. We have used no additional absorbers in front of the NaI detectors. The unfolded spectrum is given as number of transitions per 40 keV transition-energy interval. At the top of the figure the 0°/90° ratio, the anisotropy, is plotted as a function of transition energy. This ratio was obtained from the separately unfolded spectra at 0° and 90°.

Fig. 5 Unfolded NaI spectra from ^{118}Te produced via the 4n channel in the reactions $^{82}Se + ^{40}Ar$ at 157, 170 and 181 MeV and $^{110}Pd + ^{12}C$ at 50 and 75 MeV. The spectra are given as the number of transitions per 40 keV transition-energy interval.

Fig. 6 For $^{82}Se + ^{40}Ar$ at 157 MeV (light lines) and 181 MeV (heavy lines), unfolded spectra for the 4n (——), 5n (— — —) and 6n (—·—) reactions, given as the number of transitions per 40 keV transition-energy interval.

Fig. 7 Plot of excitation energy versus spin for A = 122 showing the liquid-drop and rigid-sphere yrast lines and the rotating saddle-point energy.

Fig. 8 Plot of transition energy versus spin as given by the liquid-drop model (—) and as calculated by Ragnarsson and Soroka[17] with shell corrections added •••. The results of Faessler and Ploszajcak also show the distinct increase in transition energy just below spin 30.

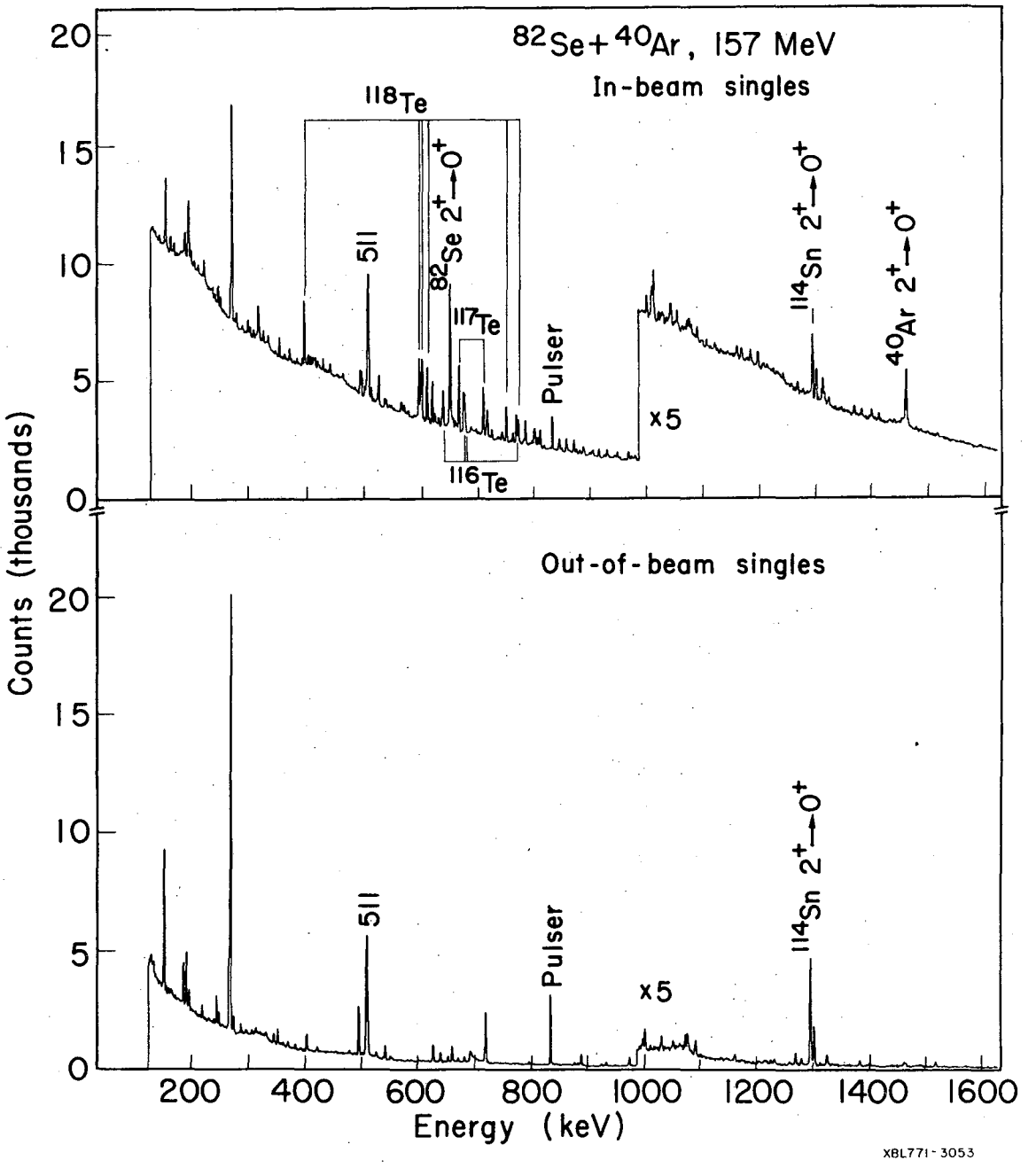
$^{82}Se+^{40}Ar$, 157 MeV
In-beam singles
^{118}Te
511
^{82}Se $2^+\rightarrow 0^+$
^{117}Te
^{116}Te
Pulser
x5
^{114}Sn $2^+\rightarrow 0^+$
^{40}Ar $2^+\rightarrow 0^+$
Out-of-beam singles
511
Pulser
x5
^{114}Sn $2^+\rightarrow 0^+$
Counts (thousands)
Energy (keV)
0
5
10
15
20
200
400
600
800
1000
1200
1400
1600
XBL771-3053

Fig. 1

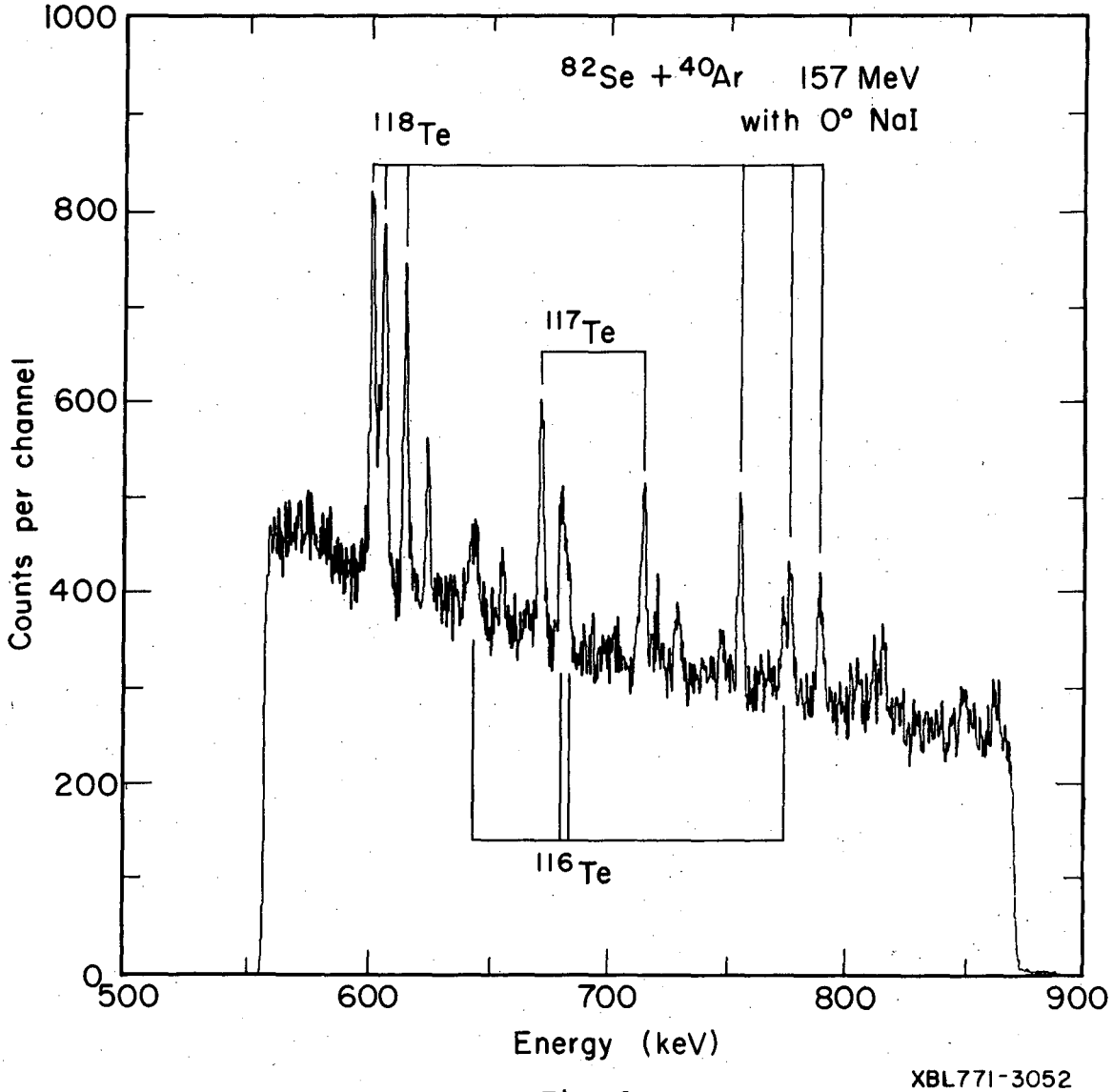

XBL771-3052

Fig. 2

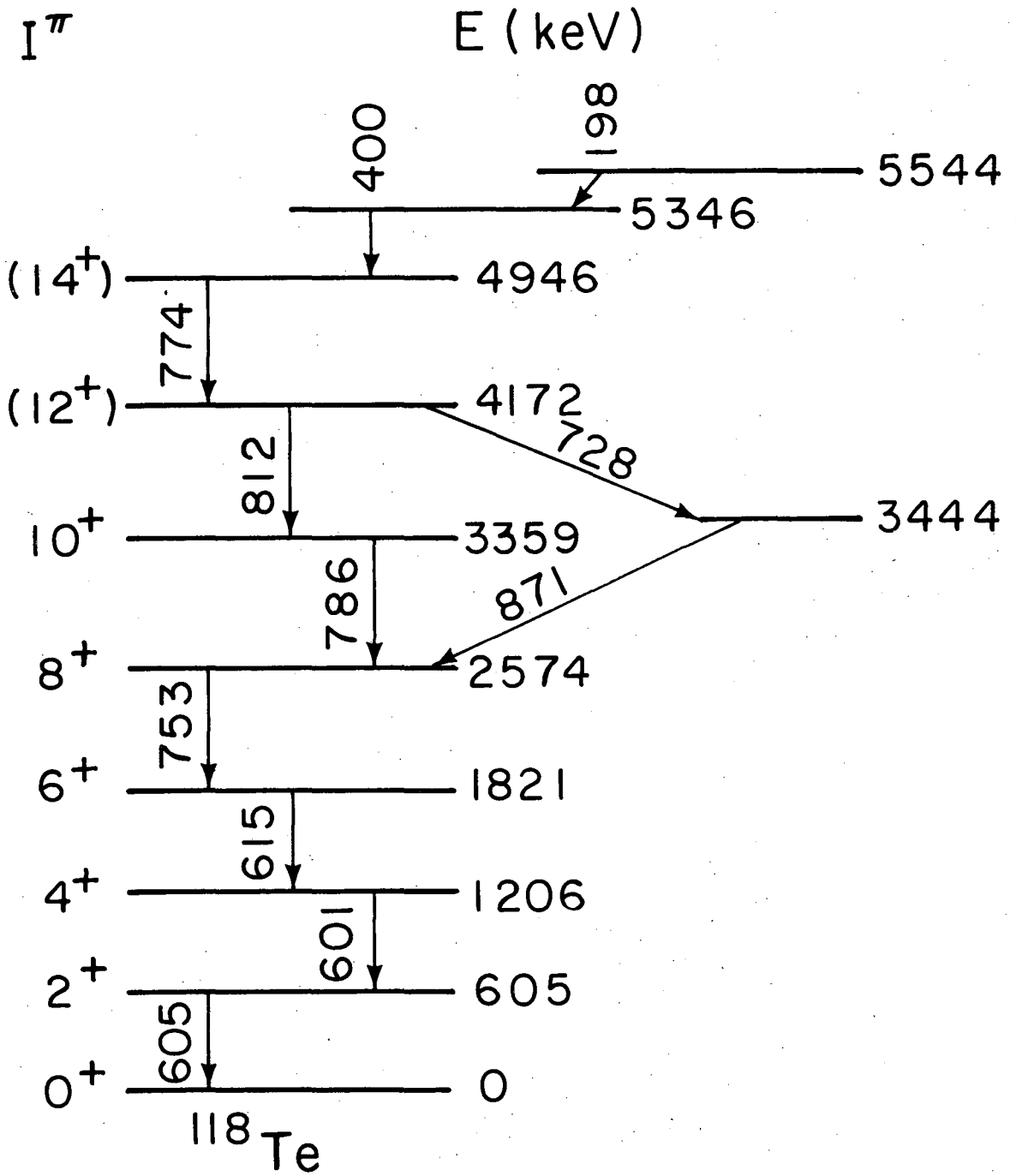

XBL771-150

Fig. 3

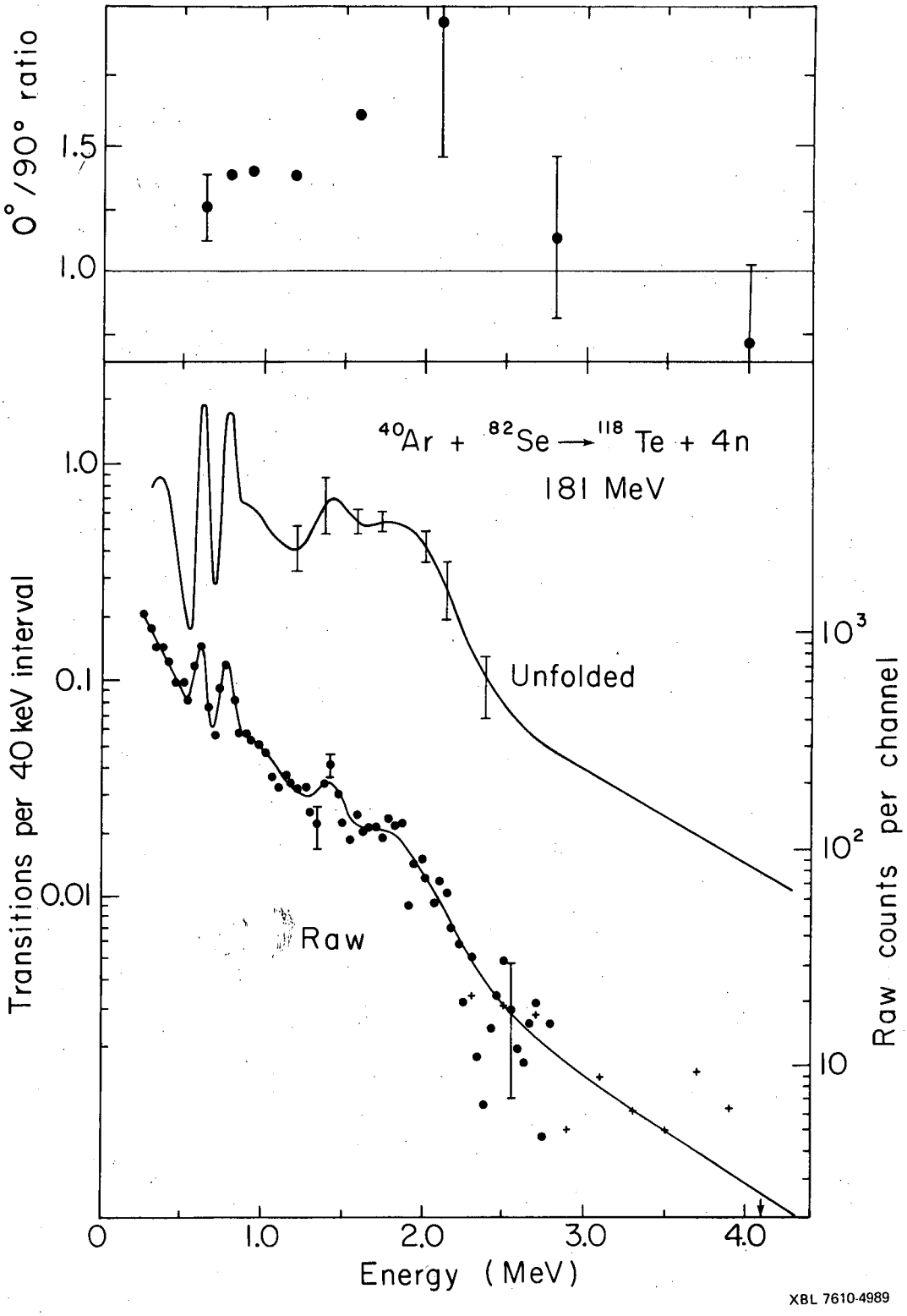

Fig. 4

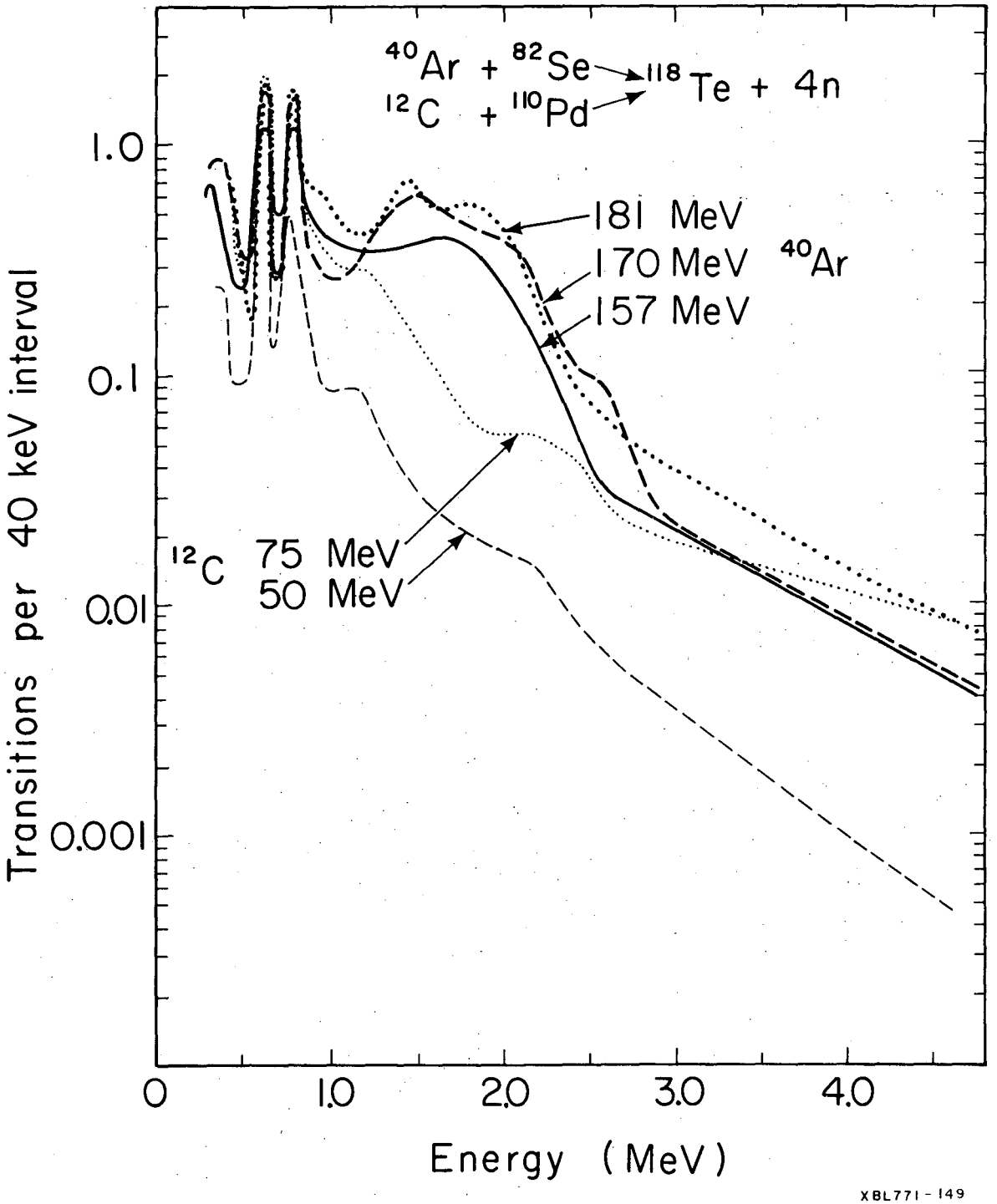
$^{40}Ar + {}^{82}Se \rightarrow {}^{118}Te + 4n$
$^{12}C + {}^{110}Pd$
181 MeV
170 MeV
157 MeV
^{40}Ar
^{12}C 75 MeV
50 MeV
Transitions per 40 keV interval
1.0
0.1
0.01
0.001
0
1.0
2.0
3.0
4.0
Energy (MeV)
XBL771-149

Fig. 5

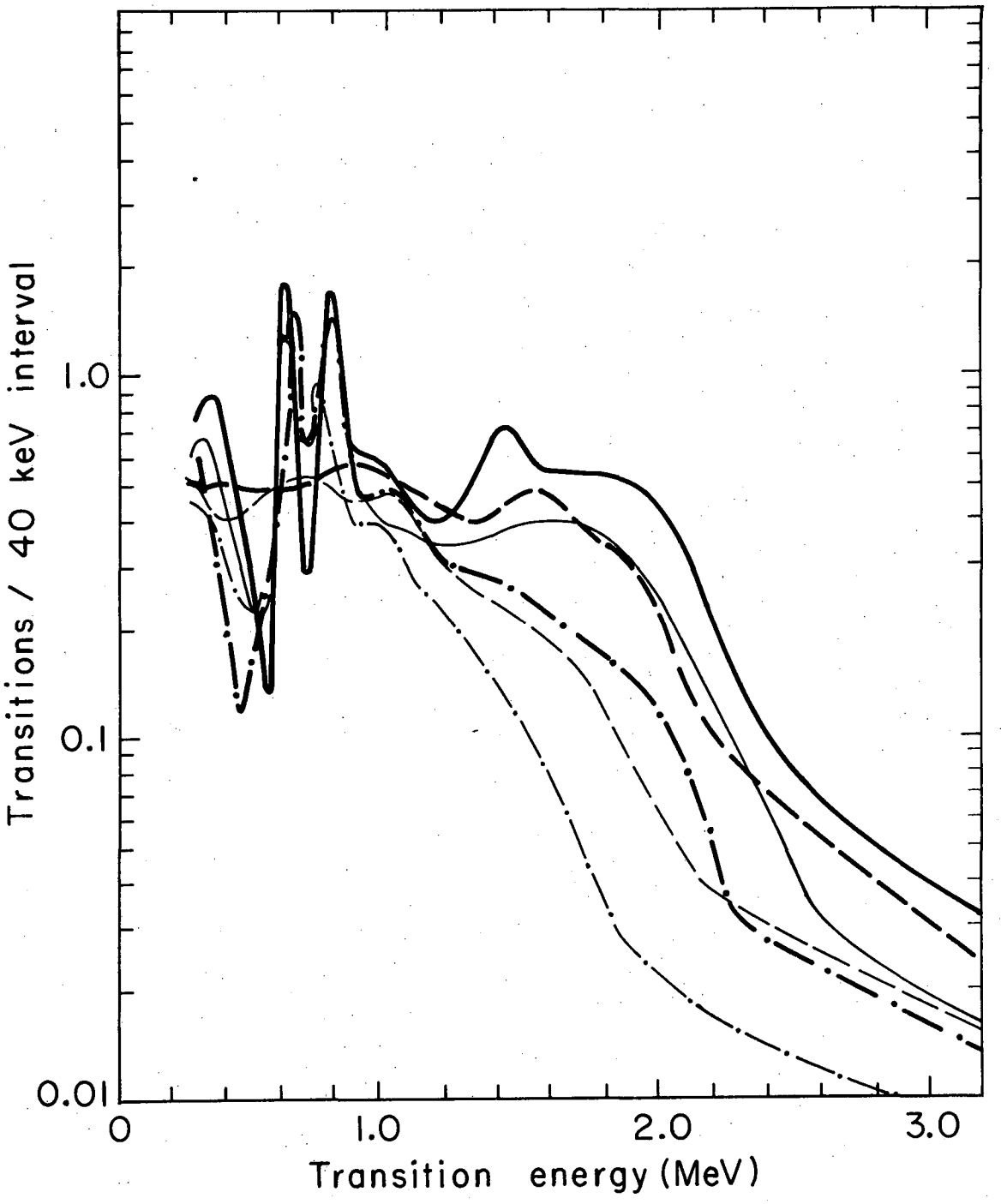

XBL 765-2847

Fig. 6

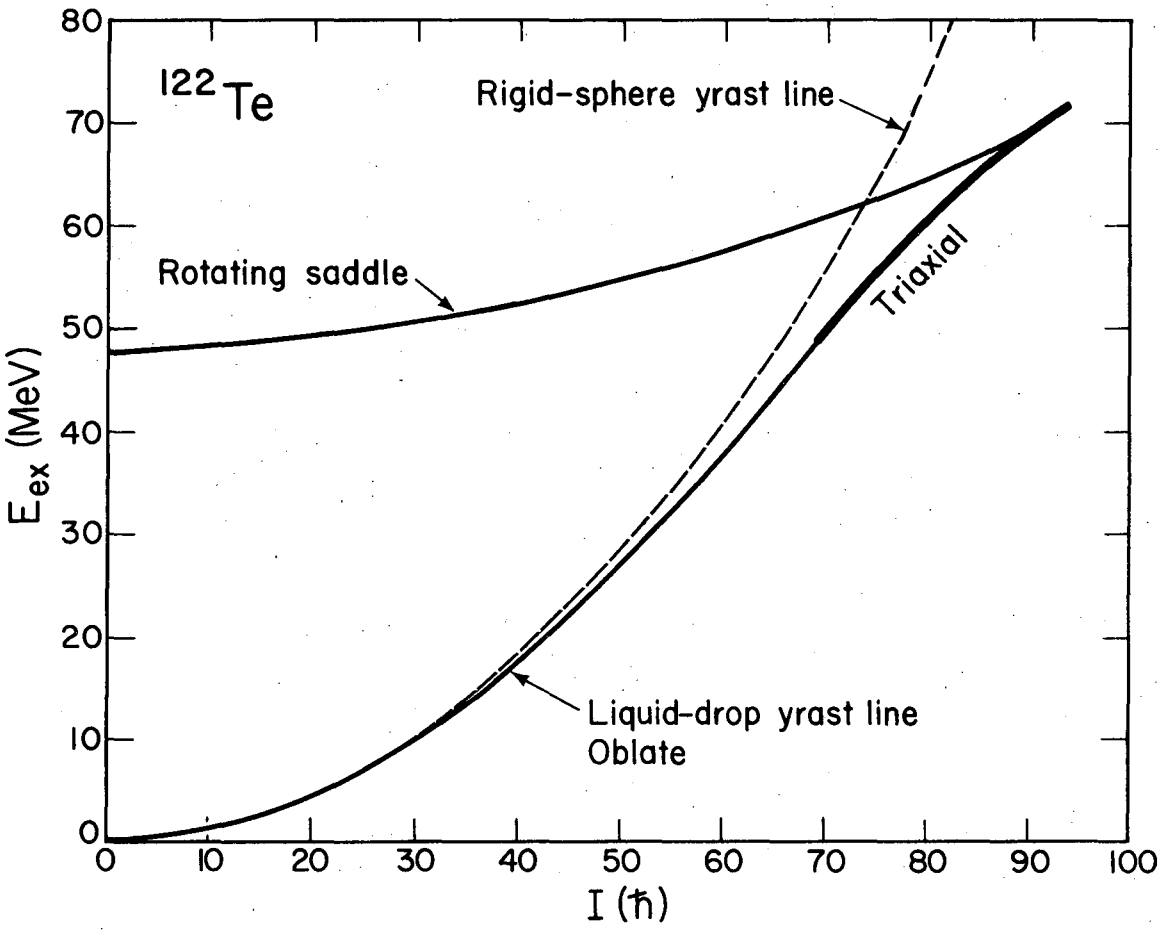

XBL 776-1081

Fig. 7

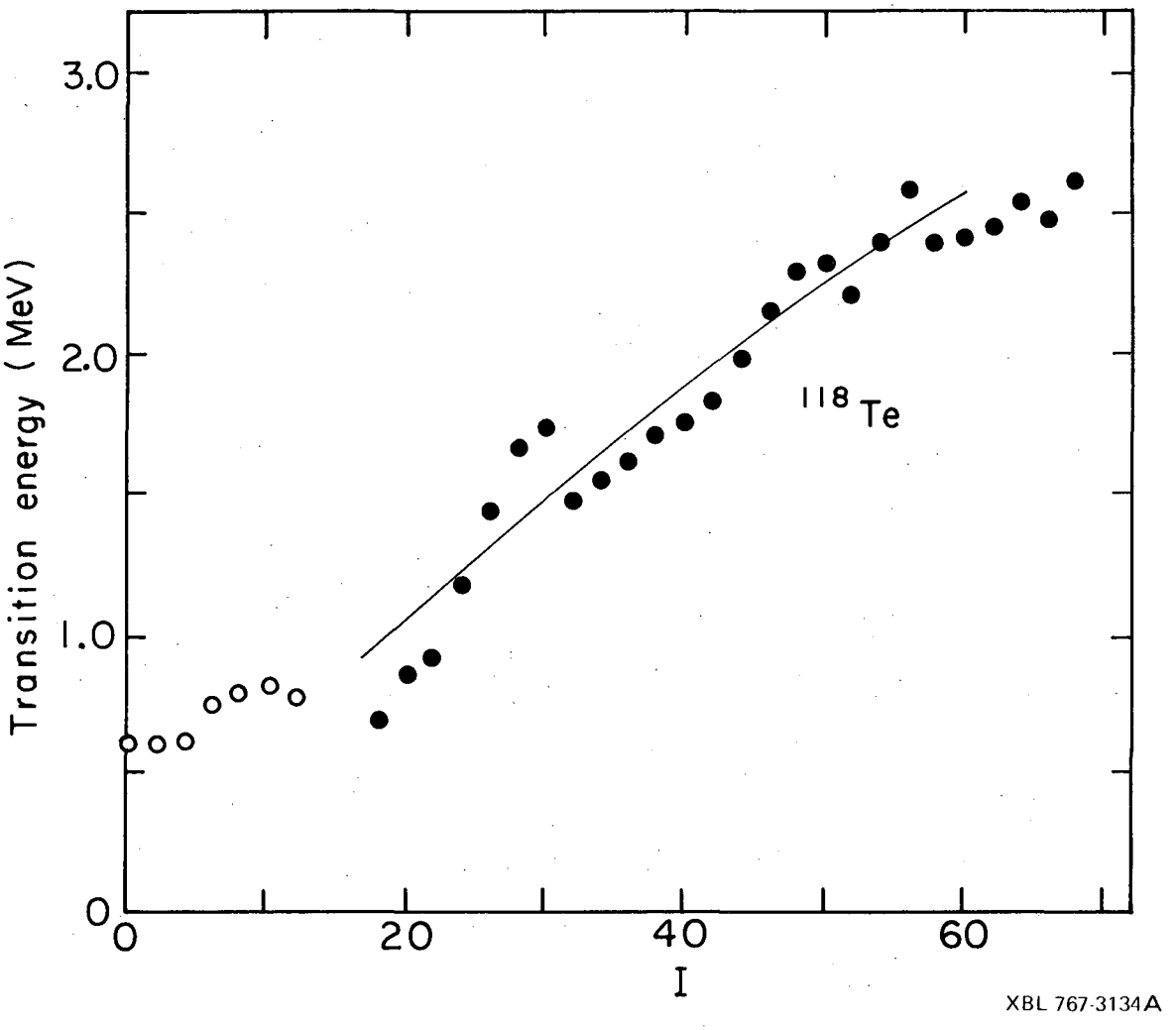
3.0
2.0
1.0
0
Transition energy (MeV)
0
20
40
60
I
118 Te
XBL 767-3134A

Fig. 8

TECHNICAL INFORMATION DEPARTMENT
LAWRENCE BERKELEY LABORATORY
UNIVERSITY OF CALIFORNIA
BERKELEY, CALIFORNIA 94720